Simple model for dry friction

J. S. Helman and W. Baltensperger*

Centro Brasileiro de Pesquisas Físicas (CBPF), Rua Dr. Xavier Sigaud 150, Rio de Janeiro, R.J. 22290, Brazil

J. A. Hołyst

Institute of Physics, Warsaw Technical University, Koszykowa 75, 00-662 Warsaw, Poland

The basis of dry friction is discussed using an independent oscillator model with longitudinal motion. This simple system is treated both numerically and with analytical methods. At vanishing velocity a sliding dry friction force is calculated which is smaller than the pinning force. At finite but not too large velocities the system displays bifurcation, chaotic motion, resonances at fractional and multiple frequencies of the oscillator, and hysteresis. Dry friction results from these complicated features. This force varies rapidly with velocity within this range, however, with a roughly constant mean value.

I. INTRODUCTION

Dissipative processes are described phenomenologically in classical equations of motions by a friction term. Usually this is assumed to be proportional to velocity.[1] This has a quantum mechanical basis, since excitations can only be created by dynamical processes.[2,3] However, dry friction, i.e., velocity independent friction, is also observed.[4] It is a force the direction of which is opposite to the velocity and with a constant absolute value while the system is moving. When the system is at rest, say, an object lying on an inclined plane, the force takes the value necessary to keep it at rest. Tomlinson,[5] in his pioneering work, noted the fact that dry friction can only appear in a composed system, such that part of it displays quick motions even when the system as a whole moves arbitrarily slowly. Several models based on this idea have been discussed,[6,7] in particular an oscillator which moves perpendicular to the gliding surface,[6] a coupled chain along this surface,[8,9] and films sliding on each other.[10] A quantum mechanical model of dry friction has been proposed in connection with experiments with the scanning force microscope.[11] A microscopic model was introduced[12] to describe dry friction in micromagnetism.[13]

In this work a single oscillator tangential to the surface is considered. This oscillator moves along the direction of the force and it is capable of lagging behind the moving system. This simple model is treated both numerically and with analytical methods. It is found that the movement presents features which have not been discussed in this context.

II. THE MODEL

Consider a system which as a whole moves with constant velocity V on a straight line. A small part of the system of mass M can move separately on that line. It is coupled to the main body by an elastic force. Its position is X, while that of the main body is Vt at time t (Fig.

1). Thus the coupling energy is

$$(M/2)\,\Omega^2(X - Vt)^2. \tag{1}$$

The small part is also subject to an external potential which can be taken to be periodic as

$$-C\cos(2\pi X/\Lambda). \tag{2}$$

While the main body moves steadily, the small object drops periodically into a potential minimum. Subsequently it is dragged out again. The motion of the main body can be arbitrarily slow, and yet the small object makes a fast motion while it is falling. This produces an energy loss by viscous friction. For the system as a whole this is an energy loss per unit distance F, which results effectively in a term of dry friction. An evaluation of the friction coefficient, $\mu = F/F_{\text{contact}}$, requires a model for the dependence of C on the contact force F_{contact}. We
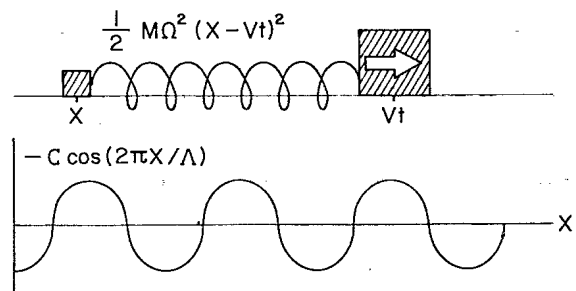

FIG. 1. Mechanical model for dry friction. The main body moves along a straight line with constant velocity V. A small object with mass M at position X is coupled through a spring of frequency Ω to the main body, and to a periodic potential $-C\cos(2\pi X/\Lambda)$. The small object drops periodically into a potential minimum and is subsequently dragged out again. The motion of the main body can be arbitrarily slow, and yet the small object moves quickly while falling. This produces an energy loss by viscous friction. The energy loss per unit distance represents a term of dry friction.

do not specify the physical interpretation of the small object, which might be a single atom capable of tangential oscillations, or a macroscopic part of the solid, say, a part of a rubber tire with this property.

III. PURE DRY FRICTION

Let the velocity V of the main body go to zero, $V \to +0$, but consider times which are large so that $Vt = L$ is finite. In this case the main body is effectively at rest during the fall of the small object into a potential minimum. At all times except during the fall the small object is in a minimum of the total potential $U(X, t)$ which is the sum of (1) and (2). The drop begins when the second derivative d^2U/dX^2 changes sign, i.e., when it vanishes. After a dropping motion the small object is again at a potential minimum. When there are several minima in $U(X, t)$, the question of where it comes to rest can only be solved using the equations of motion. Let us assume that the viscous friction is sufficiently large so that the small object comes to rest in the next minimum. In this case the following problem is to be solved: From $dU/dX = 0$ and $d^2U/dX^2 = 0$ we obtain the positions L_0 and X_0 of the system and the object, respectively, at the beginning of the drop. With the value L_0 we look for the next larger value of $X = X_1$ which satisfies $dU/dX = 0$. The energy dissipated during the drop is

$$\Delta W = U(X_0, L_0) - U(X_1, L_0). \tag{3}$$

X_0, L_0, and $U(X_0, L_0)$ can be evaluated analytically. Let

$$c = \frac{4\pi^2 C}{M\Omega^2 \Lambda^2} \tag{4}$$

be a dimensionless measure of the strength of the periodic potential compared to that of the spring; then

$$X_0 = \frac{\Lambda}{2\pi} \arccos(-1/c) , \tag{5}$$

$$L_0 = \frac{\Lambda}{2\pi} \left[\sqrt{c^2 - 1} + \arccos(-1/c) \right] , \tag{6}$$

$$U(X_0, L_0) = (c^2 + 1) M\Omega^2 \Lambda^2 / (8\pi^2). \tag{7}$$

Here $L_0 - X_0$ is positive, since $V = +0$; however, an integer multiple of Λ can be added to L_0, X_0, and X_1. $U(X_1, L_0)$ is evaluated numerically. The dry friction force F is defined as the dissipated energy per unit length, i.e., $F = \Delta W/\Lambda$. In Fig. 2 the solid line shows $f = F/(M\Omega^2 \Lambda/4\pi^2)$, as a function of $c - 1$. Note that $\Delta W = 0$ for $c < 1$, since in that case $d^2U(X, L)/dX^2 = M\Omega^2 [c \cos(2\pi X/\Lambda) + 1] > 0$, so that no instabilities can occur. It can be shown that in the range $1 < c < 4.603$ the potential U has only one minimum after the inflection point from which the drop starts. Limiting cases for the force $f(c)$ can be treated analytically with the following results:

$$f = \frac{9}{2}(c-1)^2 - \frac{18}{5}(c-1)^3 + \frac{531}{175}(c-1)^4 + O((c-1)^5)$$
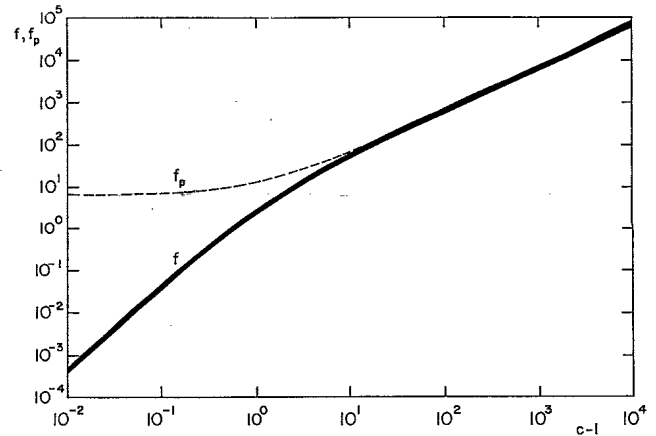
$$\text{for } c - 1 \ll 1 \tag{8}$$

FIG. 2. Dimensionless dry friction force vs $c - 1$ for arbitrarily slow motion ($v \to 0$). c is a dimensionless measure of the amplitude of the periodic potential. The dashed line represents the pinning force.

and

$$f = 2\pi c - 2\pi^2 + \frac{8}{3}\pi^{3/2} c^{-1/2} - \pi c^{-1} + O(c^{-3/2})$$

$$\text{for } c \gg 1. \tag{9}$$

Note that $M\Omega^2(L - X)$ is the external force that has to be applied to keep the velocity V constant. If the friction force at any time turns out to be larger than the available external force, the system will stop, i.e., "get pinned." This happens when the external force is less than $2\pi C/\Lambda$. When the external force reaches this limit, the spring is expanded to a length $D = L - X$ such that $M\Omega^2 D = 2\pi C/\Lambda$. In dimensionless units the corresponding force F_p becomes $f_p = 2\pi c$ which is shown in Fig. 2 by the dashed line. Once this force is overcome, the quasistatic movement of the system requires an average force $f < f_p$. The force F_p is to be identified with the so-called static friction force, while F is the sliding friction force.

One might think that the energy loss during a jump cannot exceed $2C$. This, however, is not correct. In fact, if $C \gg M\Omega^2 \Lambda^2$, when the spring jumps to the next equilibrium position at a distance of about Λ, the dissipated energy is $M\Omega^2 D \, dD \approx M\Omega^2 D\Lambda = 2\pi C$. We see that in this case it is the energy of the spring which is dissipated.

IV. DYNAMICAL TREATMENT

A dynamical treatment is required to solve the question whether the small object stops in the next minimum or proceeds further, and it is also indispensable when the system has a finite velocity. With the potentials (1) and (2) the equation of motion for the small object becomes

$$M\frac{d^2X}{dt^2} + MA\frac{dX}{dt} + \frac{2\pi}{\Lambda}C \sin\left(\frac{2\pi X}{\Lambda}\right)$$

$$+ M\Omega^2(X - Vt) = 0 , \tag{10}$$

where A is the coefficient of viscous friction. With dimensionless variables and parameters

$$x = \frac{2\pi X}{\Lambda}, \qquad \tau = \Omega t, \qquad \alpha = \frac{A}{\Omega}, \qquad v = \frac{2\pi V}{\Lambda\Omega}, \quad (11)$$

and with $\dot{x} \equiv dx/d\tau$, (10) becomes

$$\ddot{x} + \alpha\dot{x} + c\sin(x) + x - v\tau = 0. \qquad (12)$$

This nonlinear differential equation is to be solved numerically for some initial conditions $\{x(0), \dot{x}(0)\}$. Numerical solutions show that for a sufficiently large damping coefficient α, and after a time $\tau \gg 2\pi/v$, the function $x(\tau) - v\tau$ usually becomes periodic with period $2\pi n/v$ (n integer):

$$x(\tau + (2\pi n/v)) = x(\tau) + 2\pi n. \qquad (13)$$

The integer n depends on the values used for the parameters c, α, and v and the initial conditions $\{x(0), \dot{x}(0)\}$. However, the nonlinear Eq. (12) gives rise to chaos for certain ranges of the parameters c, v, and α. Figure 3 shows a phase portrait ($\dot{z}$ vs $z = x - v\tau + \alpha v$) which characterizes the oscillation. Figure 4 displays the values of $x - v\tau$ for integer multiples of periods. This stroboscopic representation makes the bifurcations and chaotic motions as a function of v apparent. One can easily see the regions of chaotic and regular solutions.

For periodic solutions the energy dissipated in an n-cycle is $\Delta W = (M\Omega^2\Lambda^2/4\pi^2)\Delta w$ where

$$\Delta w = \alpha \int_0^{2\pi n/v} \dot{x}^2 \, d\tau \qquad (14)$$

or, using the force of the spring,

$$\Delta w = \int_0^{2\pi n/v} (x - v\tau)\dot{x} \, d\tau \qquad (15)$$

or, using Eq. (13),

$$\Delta w = v \int_0^{2\pi n/v} x \, d\tau - 2\pi^2 n^2. \qquad (16)$$

A numerical evaluation can be tested by using the formulas (14)–(16), which should give the same result once a periodic solution is attained. The average force over the unit distance is $F = \Delta W/(n\Lambda)$. Figure 5 shows $f = F/(M\Omega^2\Lambda/4\pi^2)$ as a function of v. The contribution of the viscous force due to the constant velocity v is represented by the dashed line; the excess over the dashed line is the dry friction force.

V. LARGE VELOCITIES $v \gg 1$

The numerical results are rather complex. It is rewarding to note, however, that several features can be understood analytically.

Let us rewrite (12) in the form

$$\ddot{z} = -z - \alpha\dot{z} - c\sin(z)\,\cos(v\tau) - c\cos(z)\,\sin(v\tau)\,, \quad (17)$$

where $z = x - v\tau + \alpha v$ and the time τ is shifted by α. Equation (17) describes a damped harmonic oscillator which is driven parametrically by the external oscillating force $k(z,\tau) = -c\sin(z)\,\cos(v\tau) - c\cos(z)\,\sin(v\tau)$. The
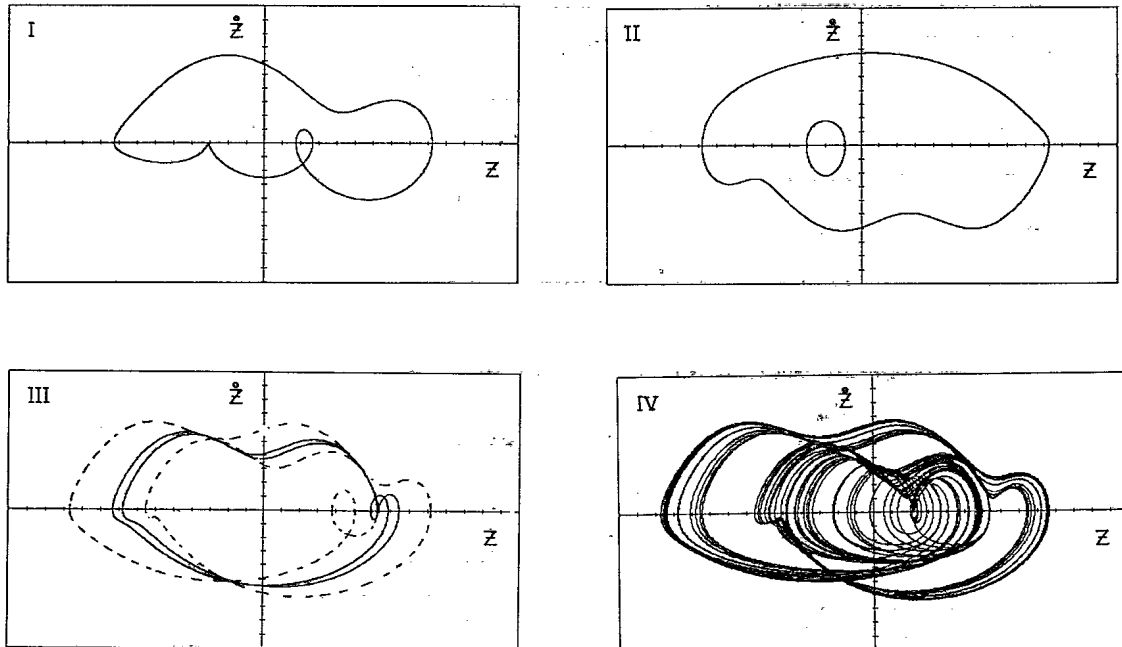

FIG. 3. Phase space representation ($\dot{z}$ vs $z = x - v\tau + \alpha v$) for $c = 4.0$ and $\alpha = 0.5$. The ranges $-7 \le z \le 7$, $-5 \le \dot{z} \le 5$ are shown. (a) Attractor with period 2 for $v = 1$. (b) A case of two attractors of period 1 (the small one) and of period 3 (the larger one) for $v = 2.995$. They are obtained starting with initial conditions $\dot{z}(0) = z(0) = 0.5$ and $\dot{z}(0) = z(0) = 0.0$, respectively. (c) Two different attractors with period 6 for $v = 2.6$. (d) Chaotic attractor for $v = 2.49$.
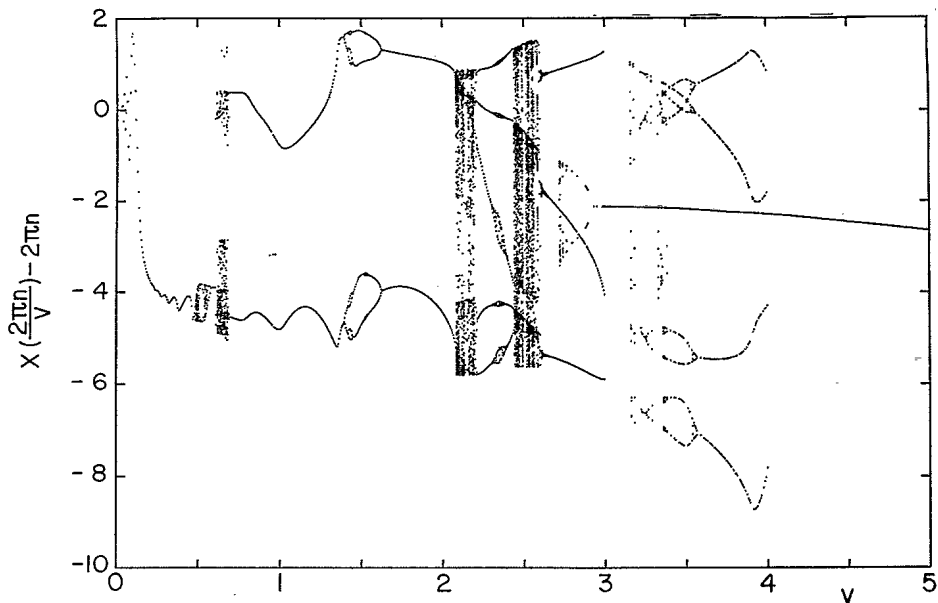
FIG. 4. Bifurcations and transitions to chaotic movements become evident in a stroboscopic plot showing $x(\tau) - v\tau$ at $\tau = 2\pi n/v$ for $n = 1, 2, \ldots, 100$, vs v $(c = 4.0, \alpha = 0.5)$.

case $v \gg 1$ corresponds to the situation when the frequency v of the external force $k(z, \tau)$ is much larger than the natural frequency of the oscillator which is equal to 1 in our units. We now apply a well known technique which is historically connected with the problem of the Kapitza pendulum.[14] We assume that the motion separates into a smooth part $\Phi(\tau)$ and a small but rapidly oscillating (with frequency v) part $\xi(\tau)$; i.e., we write $z(\tau) = \Phi(\tau) + \xi(\tau)$ where $|\xi(\tau)| \ll 1$. Expanding (17) in powers of the small parameter $\xi(\tau)$ we get up to linear terms in ξ

$$\ddot{\Phi} + \ddot{\xi} = -\Phi - \xi - \alpha\dot{\Phi} - \alpha\dot{\xi} - c\sin(\Phi)\cos(v\tau)$$
$$- c\xi\cos(\Phi)\cos(v\tau) - c\cos(\Phi)\sin(v\tau)$$
$$+ c\xi\sin(\Phi)\sin(v\tau). \qquad (18)$$

Now we separate Eq. (18) into terms that are either fast

or slowly changing in time. The fast terms satisfy approximately

$$\ddot{\xi} \approx -c\sin(\Phi + v\tau) \qquad (19)$$

because the other fast terms contain a small factor ξ, while the term $\ddot{\xi}$ is not small, since it is proportional to the large number v^2. The oscillatory solution of (19) is

$$\xi(\tau) = c\sin(\Phi + v\tau)/v^2. \qquad (20)$$

The equation for the slow variable $\Phi(\tau)$ can be obtained taking the mean value of (18) over the period $(2\pi/v)$ of fast oscillations. The result is

$$\ddot{\Phi} = -\Phi - \alpha\dot{\Phi} - \langle c\xi\cos(\Phi)\cos(v\tau)\rangle$$
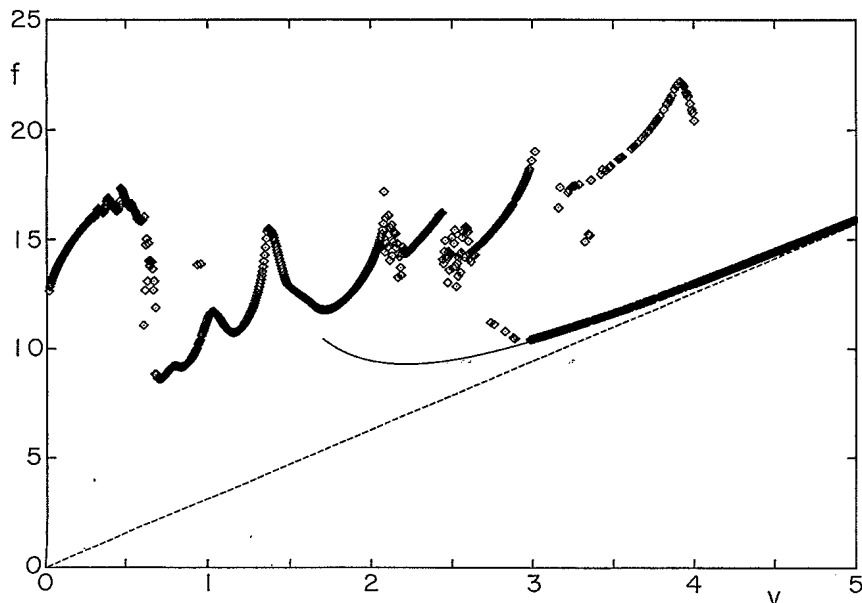$$+ \langle c\xi\sin(\Phi)\sin(v\tau)\rangle. \qquad (21)$$

FIG. 5. Average friction force $\langle f \rangle$ vs velocity v. The dashed line results from the viscous friction for constant velocity. The contribution above the dashed line is dry friction. Note that a rough average of this is essentially velocity independent in the range where dry friction dominates. The thin line is the analytic result for large velocities $v \gg 1$. The features in the figure are due to resonances, chaotic motions, nonunique attractors, and hysteresis. Here $c = 4.0, \alpha = 0.5$.

The physical meaning of the last two terms in (21) becomes evident if we use the solution (20) and write (21) in the form

$$\ddot{\Phi} = -\alpha\dot{\Phi} - \Phi - \frac{dG(\Phi)}{d\Phi} , \qquad (22)$$

where the additional "effective potential" G is a "mean kinetic energy" contributed by the fast variable,

$$G(\Phi) = \frac{\langle\dot{\xi}^2\rangle}{2} . \qquad (23)$$

From Eq. (20) then follows $G(\Phi) = c^2/(4v^2)$. Thus, in our case, $G(\Phi)$ is independent of Φ. It follows that the fast variable is decoupled completely from the slow variable in the leading order of expansion. Then, from (22), $\Phi(\tau) \to 0$ after some transient period.

For the problem of dry friction we write the average damping force as

$$f = \alpha\int_0^{2\pi/v} \dot{x}^2\,d\tau = f_{\text{visc}} + f_{\text{dry}} , \qquad (24)$$

where

$$f_{\text{visc}} = \alpha\int_0^{2\pi/v} v^2\,d\tau = 2\pi\alpha v \qquad (25)$$

and

$$f_{\text{dry}} = \alpha\int_0^{2\pi/v} \dot{z}^2\,d\tau = \frac{\pi\alpha c^2}{v^3}. \qquad (26)$$

To get the last part of (26) we put $\dot{z} \approx \dot{\xi}$ and we used (23). The leading term in the friction force (24) is f_{visc} which is proportional to the velocity v and represents standard viscous friction. The contribution of dry friction f_{dry} diminishes for large velocities as v^{-3}; it is due to the kinetic energy of the fast variable $\xi(\tau)$. The solution (24) is plotted in Fig. 5. The comparison with the numerical results shows that (24) is a very good approximation provided that initial conditions are chosen in such a way that a system evolves towards a low amplitude attractor in which it is not excited by nonlinear parametric resonance (see discussion in Sec. VI B and Sec. VI C).

VI. SMALL POTENTIAL: $c \ll 1$

There are several analytically solvable cases in the limit $c \ll 1$, i.e., when the amplitude of the periodic potential (2) is small enough.

A. Resonance at fractional frequencies

We will assume that $z = z_1 + z_2 + z_3 + \cdots$ where $z_m \sim c^m$ and $|z_m| \ll 1$. Expanding in (17) the functions $\sin(z)$ and $\cos(z)$ in series of powers of z and equating equal powers of c, we get

$$\ddot{z}_1 = -z_1 - \alpha\dot{z}_1 - c\sin(v\tau) , \qquad (27)$$

$$\ddot{z}_2 = -z_2 - \alpha\dot{z}_2 - cz_1\cos(v\tau) , \qquad (28)$$

$$\ddot{z}_3 = -z_3 - \alpha\dot{z}_3 - cz_2\cos(v\tau) + (c/2)z_1^2\sin(v\tau). \qquad (29)$$

The solution of (27) is (see the Appendix for the explicit form of all parameters)

$$z_1(\tau) = cA_1\cos(v\tau + \Delta_1). \qquad (30)$$

It possesses a standard resonance peak at $v \cong 1$. Using (30) we can write the solution of (28) as (see the Appendix)

$$z_2(\tau) = c^2[B_2 + A_2\cos(2v\tau + \Delta_2)]. \qquad (31)$$

The solution (31) possesses a resonance peak for $v \cong \frac{1}{2}$. Using (30) and (31) Eq. (29) becomes (see the Appendix)

$$z_3(\tau) = c^3[C_3\cos(v\tau + \gamma_3) + A_3\cos(3v\tau + \Delta_3)]. \qquad (32)$$

The solution (32) possesses a resonance peak for $v \cong \frac{1}{3}$.

The self-consistency of the above method requires $|z_i| \ll 1$. After some algebra we found for $\alpha \ll 1$ the following particular conditions in the neighborhood of various resonances: The resonance at $v \cong 1$ requires $c/\alpha \ll 1$, at $v \cong \frac{1}{2}$ we need $2c^2/(3\alpha) \ll 1$, and at $v \cong \frac{1}{3}$ the condition is $5c^3/(8\alpha) \ll 1$.

The contribution of the above resonances to the dry part of the friction force f becomes

$$f_{\text{dry}} = \alpha\int_0^{2\pi/v} \dot{z}^2\,d\tau \approx \pi\alpha v\sum_m c^{2m}m^2 A_m^2(v). \qquad (33)$$

To get the last part of Eq. (33) we used our solutions (30)–(32) and we neglected small contributions coming from the amplitudes B_2 and C_3. It is clear that due to the resonance form of (30)–(32) a large value of dry damping can result even from small values of the strength parameter c provided that the velocity v is near one of the resonance values $1, \frac{1}{2}, \frac{1}{3}$, etc. The comparison of the formula (33) with the numerical results is presented in Fig. 6. We have chosen such values of the parameters c and α that peaks at $v \cong \frac{1}{2}$ and $v \cong \frac{1}{3}$ can be seen easily. On the other hand for the chosen sets of parameters the condition $c/\alpha \ll 1$ is not fulfilled; this leads to evident differences between analytical and numerical results for $v > 0.6$.

B. Resonance at multiple frequencies

Besides the above resonances at fractional frequencies we observe also peaks for $v \approx 2, v \approx 3$, etc. (see Fig. 7), that follow from a combination of parametric resonances and nonlinear terms in Eq. (17). For example the presence of the parametric resonance for $v \approx 2$ can be easily understood if we linearize Eq. (17) to the form

$$\ddot{z} \approx -z - \alpha\dot{z} - c\sin(v\tau) - cz\cos(v\tau). \qquad (34)$$

Then we can use the standard theory of the parametric resonance;[1] i.e., we look for the solution

$$z(\tau) = a(\tau)\cos(v\tau/2) + b(\tau)\sin(v\tau/2) + d(\tau)\cos(v\tau)$$
$$+ e(\tau)\sin(v\tau) + g(\tau), \qquad (35)$$

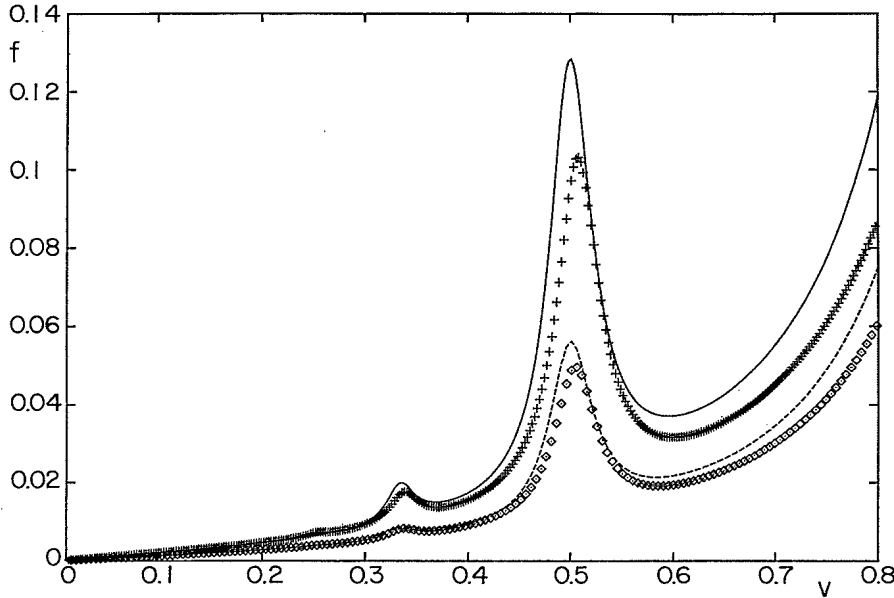where the functions $a(\tau), b(\tau), d(\tau), e(\tau), g(\tau)$ change

FIG. 6. Resonances at 1/2 and 1/3 of the frequency of the spring with $\alpha = 0.1$. $+ + +$ for $c = 0.25$, $\diamond \diamond \diamond$ for $c = 0.2$. The solid and dotted lines are the corresponding analytic approximations.

slowly in time. The result is that the coefficients $a(\tau)$ and $b(\tau)$ can grow exponentially in time provided that

$$|v - 2| < \sqrt{(c/2)^2 - \alpha^2}. \tag{36}$$

Thus the parametric resonance around $v = 2$ can appear only for

$$c > 2\alpha. \tag{37}$$

The above condition was checked with numerical data. Figure 7 displays the fact that for $c = 0.45$ and $\alpha = 0.25$ the peak around $v = 2$ disappears. In agreement with the theory we also observed in the range between $\alpha = 0.25$ and $\alpha = 0.2$ a transition from small amplitude oscillations with the frequency v to large amplitude oscillations with the frequency $v/2$ (for $v \approx 2$).

C. Hysteresis

It is interesting that for a certain range of parameters α and c several attractors can coexist [see Fig. 3(b)]. This multistability leads to the phenomenon of hysteresis: The stable solution "chosen" by the system depends on the initial conditions, i.e., on the history of the system. In our model we observed that the system behaves in a different way for increasing and decreasing velocity v (see Fig. 8), or for different initial conditions $z(0), \dot{z}(0)$ (see Fig. 3). The quantitative theory of this effect needs some approximations. We expand Eq. (17) up to terms cubic in z:

$$\ddot{z} = -\omega_0(\tau)z - \alpha\dot{z} - c\sin(v\tau) - A(\tau)z^2 - B(\tau)z^3, \tag{38}$$

where $\omega_0(\tau) = 1 + c\cos(v\tau)$, $A(\tau) = -(c/2)\sin(v\tau)$, and
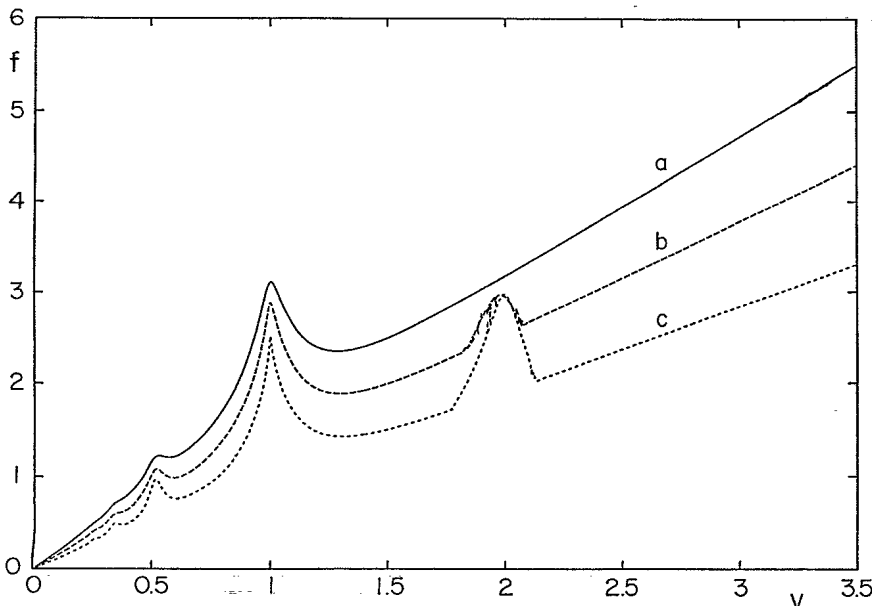

FIG. 7. Numerical data showing the influence of parametric resonance on the damping force. The resonance at $v = 2$ is subcritical for $\alpha = 0.25$ (a), while it appears for $\alpha = 0.20$ (b) and $\alpha = 0.15$ (c).
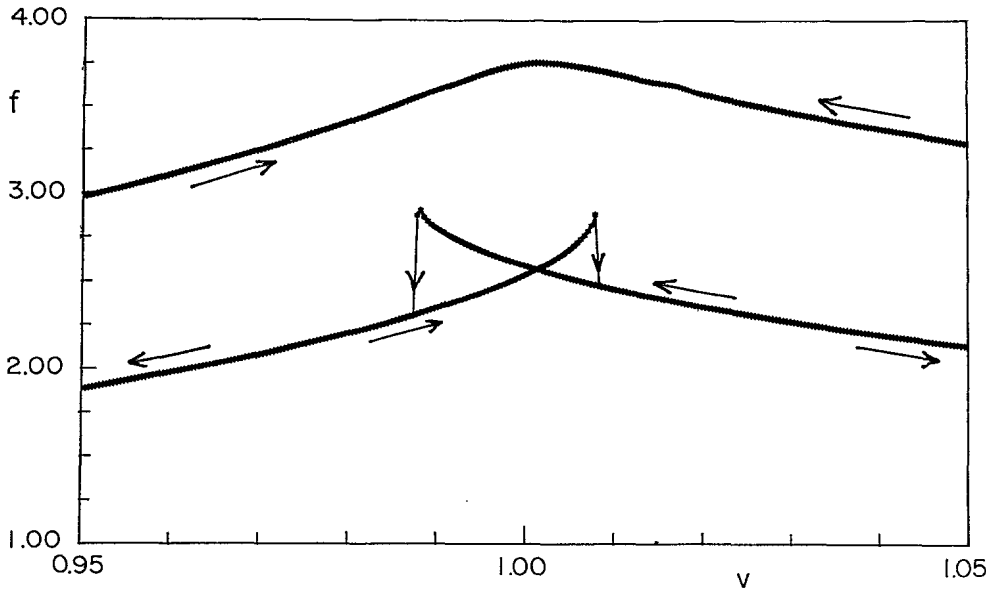
FIG. 8. Hysteresis in the dependence of the damping force on the velocity v is absent in the upper curve with $\alpha = 0.25$, while it exists for $\alpha = 0.15$ (lower curve). $c = 0.6$.

$B(\tau) = -(c/6)\cos(v\tau)$. It is well known[1] that if $A(\tau)$ and $B(\tau)$ are time independent constants, then in the case $v \cong 1$ the system described by (38) exhibits hysteresis if

$$27u^4\kappa^2 > 16\alpha^6 , \qquad (39)$$

where

$$\kappa = \frac{3B}{8\omega_0} - \frac{5A^2}{12\omega_0^3}. \qquad (40)$$

The parameter κ describes a dependence of the system eigenfrequency $\gamma = \omega_0 + \kappa b^2$ on the amplitude b of the forced oscillations. This frequency shift follows from the presence of nonlinear terms in (38). Using explicit expressions for $\omega_0(\tau), A(\tau)$, and $B(\tau)$ we calculated (up to the leading order in the powers of the small parameter c) the time averaged value $\langle \kappa^2 \rangle \cong c^2/512$. Taking into account (39) we got the following approximate condition for the presence of the hysteresis around the point $v = 1$:

$$c > J\alpha , \qquad (41)$$

with $J = 2^{1/6}4/\sqrt{3} \approx 2.59$. Table I shows numerical and analytical data for the value α_h of damping parameter α below which there is no hysteresis.

Figure 8 shows f in the neighborhood of $v = 1$ for α below and above the critical value α_h.

TABLE I. Comparison between numerical and analytical values of α_h for various values of c. α_h separates the ranges of the damping parameter α in which there is hysteresis ($\alpha < \alpha_h$) or not.

c	α_h^{num}	α_h^{an}
0.1	0.039 ± 0.001	0.0386
0.3	0.11 ± 0.01	0.116
0.6	0.21 ± 0.01	0.232
1.0	0.34 ± 0.01	0.386
2.0	0.63 ± 0.02	0.772
4.0	1.12 ± 0.02	1.54

VII. CONCLUSIONS

This work discusses a simple model of classical mechanics with the purpose to describe dry friction. The nonlinearity of the problem gives rise to a variety of complex features, such as bifurcation, chaotic motion, resonances at fractional and multiple frequencies, and hysteresis, which have been studied both analytically and numerically. Actual friction between solids may result from processes which are described by more complicated but related models. It is the aim of this work to show that even a model designed to be as simple as possible leads to a variety of phenomena which may contribute to dry friction. This is illustrated by Fig. 5 which suggests that an average over many contributions to the friction force may produce a roughly velocity independent term at not too large velocities.

ACKNOWLEDGMENTS

APPENDIX

The coefficients in the solutions (30), (31), and (32) can be written as

$$A_1 = \frac{1}{\sqrt{(1 - v^2)^2 + \alpha^2 v^2}} , \qquad (A1)$$

$$\Delta_1 = \arctan\left(\frac{\alpha v}{v^2 - 1}\right) + \frac{\pi}{2}\mathrm{sgn}(1 - v^2) , \qquad (A2)$$

$$A_2 = \frac{-A_1}{2\sqrt{(1-4v^2)^2 + 4\alpha^2 v^2}}, \qquad \text{(A3)}$$

$$\Delta_2 = \Delta_1 + \arctan\left(\frac{2\alpha v}{4v^2-1}\right) + \frac{\pi}{2}\left[\text{sgn}(1-4v^2)-1\right], \qquad \text{(A4)}$$

$$B_2 = -\frac{A_1}{2}\cos(\Delta_1), \qquad \text{(A5)}$$

$$A_3 = \frac{K}{\sqrt{(1-9v^2)^2 + 9\alpha^2 v^2}}, \qquad \text{(A6)}$$

$$K = \frac{1}{2}\left[A_2^2 + \frac{A_1^4}{16} + \frac{A_2 A_1^2}{2}\sin(\Delta_2 - 2\Delta_1)\right]^{1/2}, \qquad \text{(A7)}$$

$$\Delta_3 = \arctan(\lambda/\rho) + \arctan[3\alpha v/(9v^2-1)] + [\text{sgn}(\rho) + \text{sgn}(1-9v^2)-2]\pi/2, \qquad \text{(A8)}$$

$$\lambda = -(A_2/2)\sin\Delta_2 - (A_1^2/8)\cos(2\Delta_1), \qquad \text{(A9)}$$

$$\rho = -(A_2/2)\cos\Delta_2 + (A_1^2/8)\sin(2\Delta_1), \qquad \text{(A10)}$$

$$C_3 = A_1\sqrt{\mu^2 + \sigma^2}, \qquad \text{(A11)}$$

$$\mu = -(A_2/2)\sin\Delta_2 - (A_1^2/4) + (A_1^2/8)\cos(2\Delta_1), \qquad \text{(A12)}$$

$$\sigma = -B_2 - (A_2/2)\cos\Delta_2 - (A_1^2/8)\sin(2\Delta_1), \qquad \text{(A13)}$$

$$\gamma_3 = \arctan(\mu/\sigma) + [\text{sgn}(\sigma)-1]\pi/2 + \Delta_1. \qquad \text{(A14)}$$

* Previous address: Theoretical Physics, ETH Hönggerberg, 8093 Zürich, Switzerland.

[1] L.D. Landau and L.M. Lifshitz, *Mechanics*, 3rd ed. (Pergamon Press, Oxford, 1976), Sec. 26.

[2] L.I. Schiff, *Quantum Mechanics*, 2nd ed. (McGraw-Hill, New York, 1955), p. 213.

[3] J.E. Sacco, J.B. Sokoloff, and A. Widom, Phys. Rev. B **20**, 5071 (1979).

[4] A. Sommerfeld, *Mechanics* (Academic Press, New York, 1952), Sec. 14.

[5] G.A. Tomlinson, Philos. Mag. **7**, 905 (1929).

[6] G.M. McClelland, in *Adhesion and Friction*, edited by M. Grunze and H.J. Kreuzer, Springer Series in Surface Science Vol. 17 (Springer-Verlag, Berlin, 1990), p. 1.

[7] G.M. McClelland and J.N. Glosli, in *Fundamentals of Friction: Macroscopic and Microscopic Processes*, edited by

I.L. Singer and M. Pollock, Vol. 220 of *NATO Advanced Study Institute, Series E: Applied Sciences* (Kluwer, Dordrecht, 1992), p. 405.

[8] Y.I. Frenkel and T. Kontorova, Zh. Eksp. Teor. Fiz. **8**, 1340 (1938).

[9] J.B. Sokoloff, Phys. Rev. B **42**, 760 (1990).

[10] James N. Glosli and Gary M. McClelland, Phys. Rev. Lett. **70**, 1960 (1993).

[11] W. Zhong and D. Tománck, Phys. Rev. Lett. **64**, 3054 (1990).

[12] W. Baltensperger and J.S. Helman, J. Appl. Phys. **73**, 6516 (1993).

[13] J.A. Hołyst, W. Baltensperger, and J.S. Helman, Solid State Commun. **82**, 763 (1992).

[14] Reference [1], Sec. 30.